Phase effects owing to multilayer coatings in a two-mirror extreme-ultraviolet Schwarzschild objective

Edita Tejnil, Kenneth A. Goldberg, and Jeffrey Bokor

The aberrations of a multilayer-coated reflective Schwarzschild objective, which are influenced both by mirror surface profiles and by multilayer coatings, are evaluated with a phase-shifting point diffraction interferometer operating in the extreme ultraviolet. Using wave-front measurements at multiple wavelengths near 13.4 nm, we observed chromatic aberrations and wavelength-dependent transmission changes that were due to molybdenum–silicon multilayer coatings. The effects of chromatic vignetting due to limited multilayer reflection passbands on the imaging performance of the Schwarzschild optic are considered. The coating characteristics extracted from the interferometry data on the two-mirror optical system are compared with previously reported coating properties measured on individual mirror substrates. © 1998 Optical Society of America

OCIS codes: 230.4170, 260.7200, 120.3180, 120.5050, 230.4040.

1. Introduction

Wave-front characterization at the operational wavelength plays a key role in the development of near-diffraction-limited optical systems. Interferometric measurements of reflective multilayer-coated optics operating at extreme-ultraviolet (EUV) wavelengths reveal the overall system wave front, influenced not only by the physical geometry of the mirror surfaces but by angle-dependent phase shifts in the multilayer coatings. A phase-shifting point diffraction interferometer[1] for wave-front measurements at EUV wavelengths has been implemented at the Advanced Light Source at the Lawrence Berkeley National Laboratory. The interferometer has been used for evaluation of the wave-front aberrations in a reflective, 10×-demagnifying, multilayer-coated Schwarzschild objective at wavelengths near 13 nm.[2,3] Owing to the fact that, on a change in wavelength, the contribution to the wave-front aberrations from multilayer phase shifts changes whereas that which is due to purely geometric errors does not,[4] multilayer effects can be observed directly by means of wave-front measurements over a range of wavelengths.

In this paper we report on the measurements of the wavelength-dependent multilayer coating effects in the two-mirror Schwarzschild objective with point diffraction interferometry. The chromatic aberrations in the Schwarzschild optic that are due to molybdenum–silicon (Mo/Si) multilayer reflective coatings are characterized near 13.4-nm wavelength, and their effect on image quality is also considered. Furthermore, the measurements of the wavelength-dependent reflectivity and phase of the assembled two-mirror system are compared with calculations based on the ideal optical and multilayer coating designs as well as with calculations based on independent measurements of the multilayer period of the individual mirrors.[5]

2. Interferometry Measurement

The phase-shifting point diffraction interferometer for at-wavelength testing of EUV optics operates at undulator beam line 12.0 at the Advanced Light Source at the Lawrence Berkeley National Laboratory. The undulator source provides high-brightness, EUV radiation tunable from 5 to 25 nm in wavelength and linearly polarized with the electric field vector in the horizontal plane. The FWHM spectral bandwidth of the radiation used in these experiments is roughly 0.05 nm. The grazing-incidence beam-line optics include a grating mono-

When this research was performed, the authors were with the Center for X-Ray Optics, Lawrence Berkeley National Laboratory, Berkeley, California 94720. E. Tejnil and J. Bokor were also with the Department of Electrical Engineering and Computer Sciences, University of California, Berkeley. E. Tejnil is currently with Intel Corporation, Santa Clara, California 95052. K. A. Goldberg was also with the Department of Physics, University of California, Berkeley.

Received 2 February 1998; revised manuscript received 27 April 1998.

0003-6935/98/348021-09$15.00/0

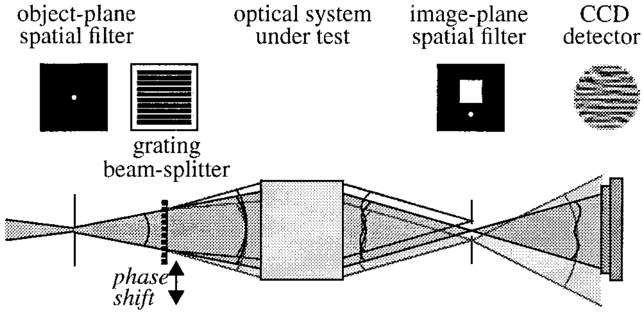

Fig. 1. Components of the phase-shifting point diffraction interferometer for characterization of the multilayer-coated Schwarzschild optical system.

chromator, used to select the desired wavelength and spectral bandwidth, and a Kirkpatrick–Baez illuminator, designed for optimum transfer of spatially coherent radiation to the interferometer.

The phase-shifting point diffraction interferometer for testing the aberrations in the Schwarzschild optical system is illustrated schematically in Fig. 1. The interferometer design,[1] based on the properties of light diffracted from small pinhole apertures, is suited for highly accurate measurements of wave-front aberrations over a wide range of wavelengths. The optic under test is illuminated by a spatially coherent spherical wave front diffracted from a pinhole source placed in the object plane of the test optic. To ensure a high-quality illumination wave-front that is spherical across the solid angle accepted by the entrance numerical aperture of the optic, the entrance pinhole must be smaller than the diffraction-limited spot size resolvable by the test optic on the object side. We refer to such a pinhole as a subresolution pinhole. A coarse diffraction grating, placed between the object-plane pinhole and the Schwarzschild optic, serves as a small-angle beam splitter by dividing the wave front into multiple diffractive orders. On propagation through the test optic, the perfect illumination wave fronts become aberrated because of errors in the optical system under test. Two of the diffractive orders are selected with a two-pinhole spatial filter placed in the image plane of the optic. The zero diffractive order is chosen as the test beam and transmitted through a window, which is significantly larger than the focal spot size. One of the first diffractive orders is spatially filtered by a subresolution pinhole to produce a spherical reference wave front over the numerical aperture of the measurement. The choice of the zero diffractive order for the test beam ensures that aberrations that are due to the grating line placement are not introduced into the measured wave front. Translation of the grating in the direction perpendicular to its lines controls the relative phase shift between the test and the reference beams that is necessary for phase-shifting interferometry. The interference of the test and the reference beams is recorded with a charge-coupled device detector. A detailed description of the interferometer configuration for testing this Schwarzschild optic is given elsewhere.[2] The rms precision of this apparatus in characterizing the overall wave-front error in the optic was found to be 0.11 nm. Its sensitivity to small changes in the wave front with the illuminating wavelength is considerably greater because it can be examined without the need for mechanical motion of any of the critical interferometer components.

The Schwarzschild objective test optic designed for 10×-reduction EUV projection lithography experiments consists of two nearly concentric spherical mirrors.[6] Both mirrors are coated with Mo–Si multilayer reflective coatings with peak reflectivity near 13.4-nm wavelength. The annular, concave secondary is coated with a multilayer of nearly uniform thickness; the convex primary has a graded multilayer coating designed to compensate for the varying angles of incidence across its surface.[5,6] An off-axis aperture stop that rests upon the primary mirror is intended to select an unobstructed circular portion of the annular clear aperture when it is used for imaging experiments [Fig. 2(a)]. The 10× demagnifying system has a numerical aperture (NA) of 0.08 and a corrected field of view 400-μm in diameter in the image plane. The NA of the system is adjustable with a rotatable aperture stop that contains three separate subapertures that correspond to selectable numerical apertures of 0.06, 0.07, and 0.08, referred to as C, A, and B, respectively. The image plane of the optic, determined during the assembly of the system, is defined by three balls attached to the optical housing. The object plane is not mechanically referenced to the optical housing.

3. Wavelength-Dependent Transmission and Phase

In the characterization of the two-mirror 10× Schwarzschild optic, both the transmitted intensity and the wave-front phase were measured at several EUV wavelengths within the central transmission lobe of the multilayer coatings, ranging from approximately 12.9 to 13.7 nm (null to null) with a peak near 13.4-nm wavelength. The transmission through subaperture A of the optic (with a NA of 0.07) is shown in Fig. 2(b) at wavelengths of 13.0, 13.2, 13.4, and 13.6 nm. The transmission through different portions of the off-axis subaperture reveals a zonal effect that follows the annular full aperture of the optic. Near the center of the coating passband, at 13.2 and 13.4 nm, the transmission is quite uniform; it is lower only near the edges of the annulus. The measured transmission along the center of the annulus is peaked at 13.37-nm wavelength, nearly in agreement with the coating design,[5] but the transmission peak is shifted to 13.30 nm on the inner edge of the annulus and to 13.36 nm on the outer edge of the subaperture. These shifts indicate that the multilayer coating period deviates from its intended value that was designed to achieve a reflectivity uniformity of better than 99% at 13.4 nm. At the edges of the coating reflectance passband, at 13.0 and 13.6 nm, the transmission is nonuniform. This behavior is not unexpected, even for perfect multilayers, be-

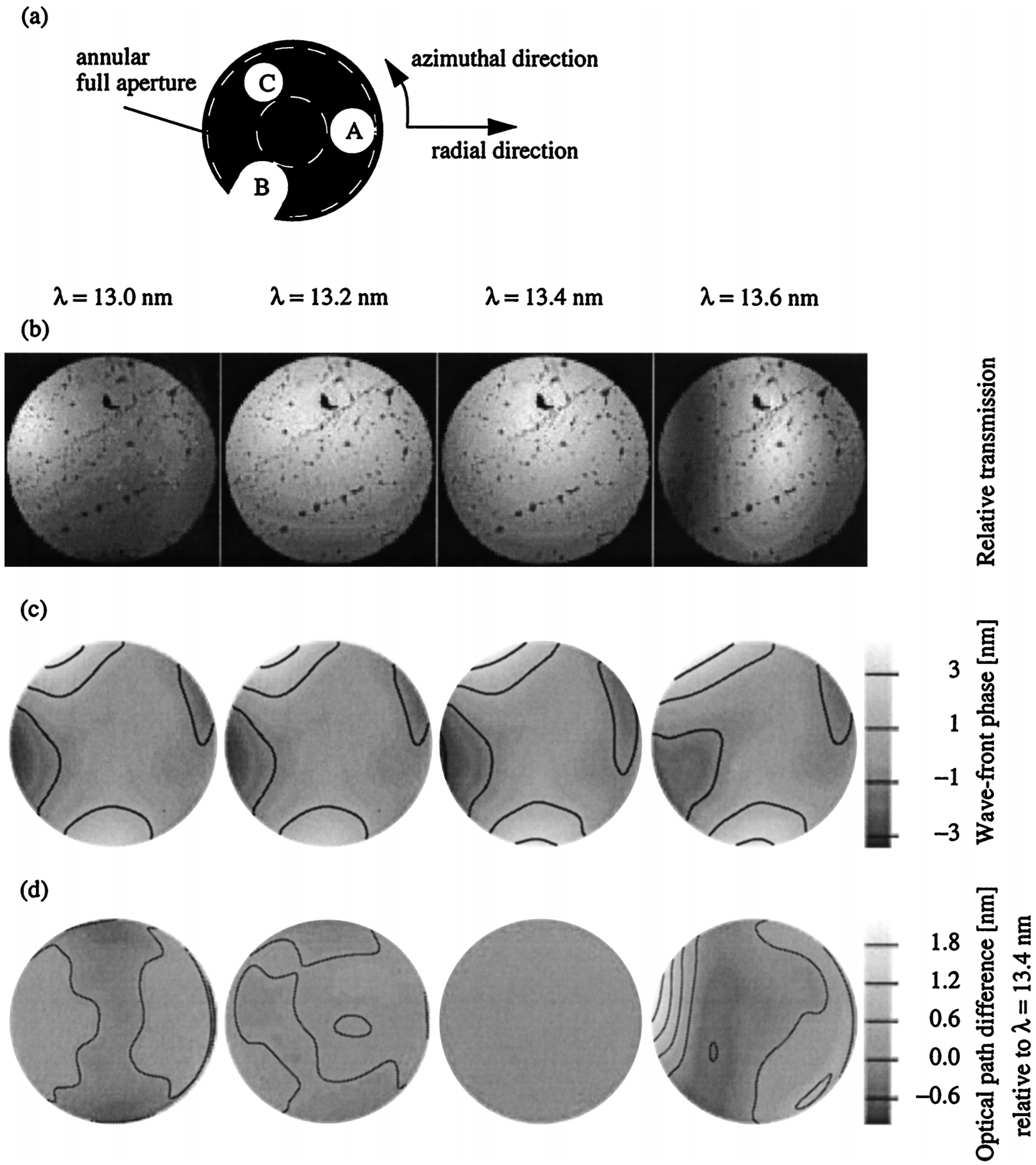

Fig. 2. Measured chromatic effects produced by multilayer reflective coatings. (a) Schematic representation of the subapertures selecting portions of the annular full aperture of the Schwarzschild optic. As the wavelength is changed, (b) the transmission and (c) the wave-front phase vary in subaperture A. The transmission peak is near 13.4-nm wavelength. (d) The measured differences between the aberrations at the indicated wavelengths and the 13.4-nm wavelength demonstrate the presence of multilayer coating phase aberrations.

cause the coatings are designed to accommodate a range of incidence angles in a limited spectral band. Outside the design passband, the differences in incidence angles across the optic are amplified because the coating properties vary rapidly outside the central reflectivity lobe.[5]

The phase of the wave front transmitted through subaperture A at 13.0, 13.2, 13.4, and 13.6 nm is displayed in Fig. 2(c). The phase maps are found from phase-shifting analysis of several data series from the phase-shifting point diffraction interferometer.[7] The phase excludes the piston and tilt terms that are not measured by interferometry but contains the defocus that contributes to the chromatic aberrations. The chromatic phase effects that result from reflection by the two multilayer mirrors are illustrated in Fig. 2(d), which shows the differences between aberrations measured at 13.0, 13.2, 13.4, and 13.6 nm and aberrations measured at 13.4 nm. Within the coating passband, the differences in the measured wave fronts are small because the wavelength change results primarily in a constant phase offset, which is not detected in this experiment. At the passband edges, where nonuniformities in the coating properties are accentuated, the measured phase difference over the aperture is consistent with an imperfection in the multilayer coating thickness that varies along the radius of each mirror.

The rms difference between the wave front measured at various wavelengths and the aberrations at 13.4 nm is given in Fig. 3(a). This aberration difference, which includes changes in the focus with wavelength, illustrates the magnitude of the chromatic aberrations in the Schwarzschild objective. The wavelength-dependent change in the tilt term produced by the optic, which is not detected in this experiment but can in principle cause chromatic image distortion, is not expected to be of significant magnitude. Based on calculations that utilize the measured period of the multilayer coatings,[5] the change in the tilt relative to 13.4-nm wavelength is quite small over the wavelength range measured. The measured chromatic aberrations with the calculated wavelength-dependent tilt term added are also given in Fig. 3(a). The relative transmission of different radiation wavelengths through subaperture A is plotted in Fig. 3(b). The largest measured wave-front change, approximately 0.44 nm rms, equivalent to 0.033 wave at 13.4-nm wavelength, occurs at a wavelength near 13.6 nm, where the overall transmission through the optic is reduced by an order of magnitude relative to the peak. The wavelength-dependent tilt increases the aberration difference somewhat, but only outside the main transmission lobe. Our overall conclusion is that the chromatic aberrations are not expected to degrade the image quality appreciably for this Schwarzschild optic.

In EUV multilayer-coated optical systems the fraction of the optical power near the edges of the reflectivity passband is likely to be quite small because of the reduced reflectivity of the multilayer coatings, especially when multilayer-coated condenser optics are employed. Although the chromatic aberrations are determined by the optical design and by the properties of the deposited coatings, their effect on the image quality may be negligible, provided that most of the optical power resides within the transmission passband of the imaging system.

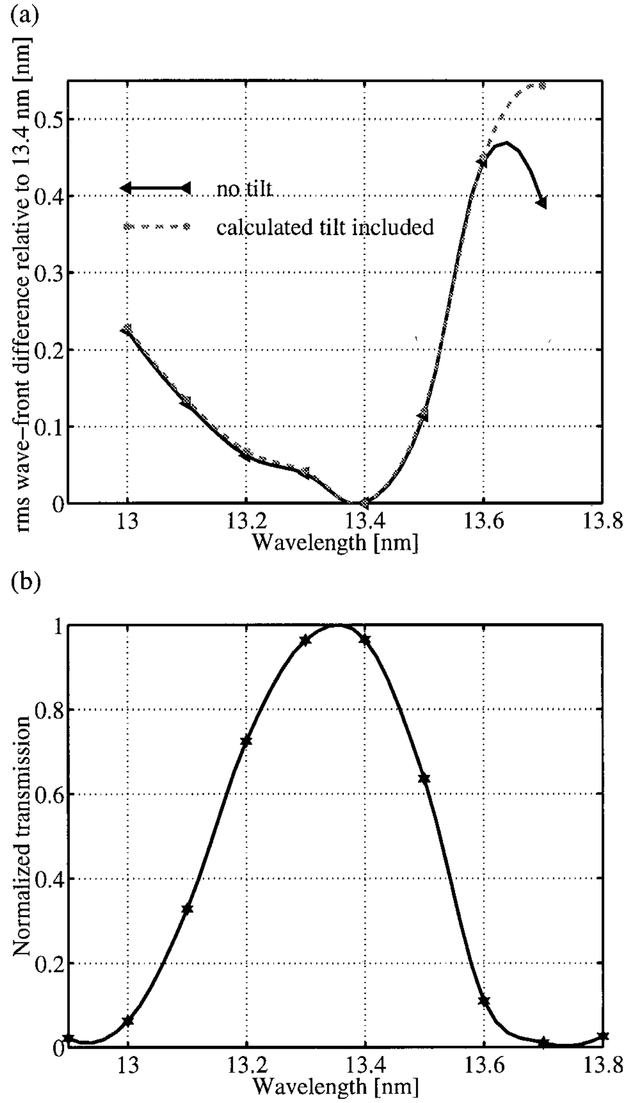

Fig. 3. (a) The chromatic aberrations of the 0.07-NA subaperture of the Schwarzschild objective are revealed in the measured rms difference between the wave fronts at different wavelengths and the wave front at 13.4 nm. (b) Overall normalized transmission through the 0.07-NA subaperture measured as a function of wavelength.

4. Understanding the Measured Coating Properties

One can use the chromatic reflectivity and phase effects to evaluate the properties of the Mo–Si multilayer coatings on the two Schwarzschild mirrors. In this section, we compare the measured wavelength dependence with the changes in the transmission and the phase calculated from the designed and the previously measured properties of the multilayer coatings that were reported in Ref. 5. The reported multilayer coating period corresponds to measurements made of several sets of mirrors of the same type, fabricated at the same time, one of which was used in assembling the Schwarzschild optics discussed here. The Mo–Si coatings consist of 40 bilayers with a molybdenum-to-silicon thickness ratio of ~0.375. The multilayer coating period varies with radial position on each mirror substrate. On the convex primary mirror, the multilayer coatings are graded in thickness and the 0.08-NA aperture stop (subaperture B) selects the radial positions of 3.3–7.3 mm in the annular aperture. On the concave secondary mirror, with nearly uniform multilayer period, the annular clear aperture ranges from 16.5 to 41.0 mm in radius. Refractive indices of coating materials are determined from tabulated optical properties at x-ray wavelengths[8] by use of specific densities of 10.22 for molybdenum and 2.33 for silicon.

In addition to the coating properties, the calculation of the multilayer effects in the optical system also utilizes the optical design for the Schwarzschild optic.[6] In the consideration of multilayer properties, the mirror surface figure errors are neglected because they do not significantly alter the position and orientation of the mirror surface. Unless indicated otherwise, the illumination of the optic from a field point on the optical axis is assumed. Although the multilayer effects depend on the polarization, only the transverse-electric polarization need be considered here because the beam in the interferometer experiment is initially transverse-electric polarized and only a small fraction of the total reflected light is coupled into the transverse-magnetic polarization in propagation through the system.[9] The multilayer calculations employ the successive application of the Fresnel equations[10–12] and include the effects of graded layer interfaces. The layer interface grading was modeled with an error function profile described by a rms interface thickness σ. This model for the interfaces reduces the amplitude reflectivity at each interface by the Debye–Waller factor,[11,13] which decreases exponentially with σ^2.

The variations in the transmission properties within subaperture A are examined in Fig. 4. The transmission measured in the course of the interferometry experiments is plotted in Fig. 4(b) as a function of wavelength for five small regions of the subaperture that are indicated in Fig. 4(a). The measured transmission is compared in Fig. 4(c) with the calculated transmission curves for the multilayer coating period from Ref. 5. This computation assumes a layer interface thickness of 0.7 nm in the multilayer, representative of the Schwarzschild mirrors, and an ideal optical design with the object point at the center of the field of view. Although reflectance data are not available for the Schwarzschild mirror coatings, measurements of similar multilayers upon flat substrates indicate reflectivities of 63–65% near normal incidence.[14,15] Assuming that characteristics of the multilayers deposited under similar conditions are representative of the Schwarzschild mirrors, the near-normal-incidence reflectances of 63–65% correspond to a rms interface thickness of roughly 0.7 nm.

Our measurements of the coating properties reveal nonuniformities along the radial direction of the annular full aperture and nearly constant transmission only in the azimuthal direction. Relative to the center of the annulus, the transmission peak is shifted toward shorter wavelengths at both the inner and the outer edges. In regard to variations over subaperture A, the transmission measured here and that calculated by use of the reported multilayer period[5] are in good qualitative agreement. In addition to a small offset in the peak wavelengths, the most apparent discrepancy between the two is the transmission bandwidth. The measured FWHM bandwidth is ~85% of that predicted from the calculations. The design bandwidth is larger than either measurement because of the reduction in the multilayer transmission bandwidth from imperfections that result from interdiffusion and roughness at the layer boundaries.

The transmission properties along the radial direction of the annulus are summarized in Fig. 5, with plots of the transmission curve center (midpoint between the FWHM wavelengths) in Fig. 5(a) and of the

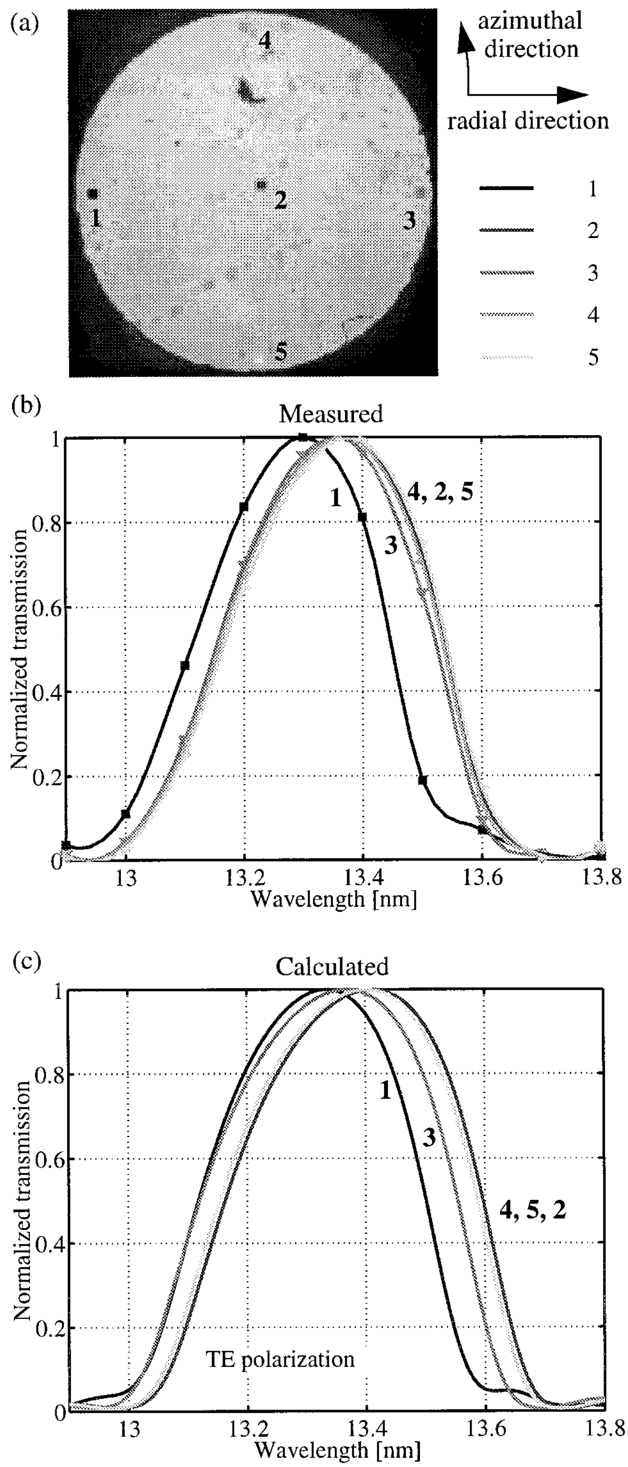

Fig. 4. (a) Transmission through the Schwarzschild optic versus wavelength at the indicated positions within the 0.07-NA subaperture. (b) Measured transmission curves compared with (c) the calculation that uses the multilayer periods measured in Ref. 5. The calculation assumes multilayer interfaces with 0.7-nm interface thickness.

bandwidth in Fig. 5(b). The radial coordinate corresponds to scaled radial positions relative to a 0.08-NA pupil with a normalized radius of 1. The results are given for the ideal multilayer design, for the calcula-

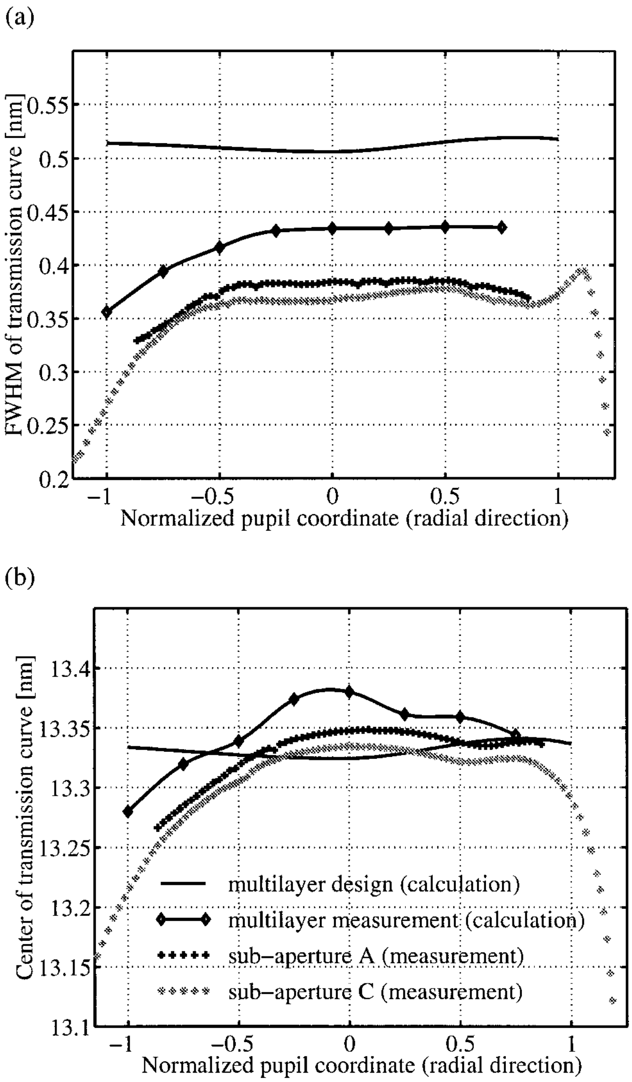

Fig. 5. (a) Center and (b) FWHM bandwidth of the transmission passband for the 10× Schwarzschild optic. Calculations based on the multilayer design and on previously reported multilayer period measurements are compared with measurements in two different portions of the annular aperture of the Schwarzschild optic.

tion that uses the previously measured multilayer periods with 0.7-nm layer interface thickness, and for two different parts of the annulus measured here. The measurements in the regions of subapertures A and C of the annulus demonstrate comparable properties in the azimuthal direction, as expected.

The discrepancy between the measurement and the measurement-based calculation of the coating bandwidth has numerous possible explanations in a complex multilayer system with several curved mirrors and graded-period multilayer coatings, possibly illuminated from several directions. The potential causes of this discrepancy explored here include the illumination of the optic from different field points, the imperfections of multilayer interfaces, and the mismatch in the passbands of the two Schwarzschild mirrors.

As we mentioned above, the object plane of the Schwarzschild optic is not mechanically referenced to the optical housing. One selects object positions within the field of view by steering the beam through the center of the image plane as defined by three balls on the optical housing. This method places the beam near the center of the intended field of view in the object plane. However, a displacement of the object pinhole from its desired position with respect to the optic changes the angles of incidence on the multilayers and can potentially affect the coating reflectance. The effect of the object position on the transmission through the optic was calculated over an object-side field of view of 12 mm × 12 mm, which is three times wider than the designed field of view. Based on these calculations, the off-axis displacement of the object pinhole, estimated to be well within a 12 mm × 12 mm field in the experiment, does not account for the reduced bandwidth observed experimentally.

A mismatch of the transmission passbands of the two separate mirrors in the Schwarzschild objective can also decrease the overall multilayer bandwidth. A simple model of the coating mismatch, given by a constant offset in the multilayer period on each mirror, is investigated in Fig. 6, under the assumption of sharp layer interfaces. The multilayer periods of the 40-bilayer coating are assumed to be shifted as indicated from the values reported in Ref. 5. The transmission curve properties along the radial direction of the annular aperture are illustrated for two cases that are found to exhibit good agreement with the measured center wavelength of ~13.35 nm [see Figs. 6(a) and 5(a)]. In both cases, the multilayer period is offset by 0.055 nm on one mirror and by −0.085 nm on the other mirror. When the multilayer period on the secondary mirror is increased and that on the primary is decreased, rather than vice versa, the calculated bandwidth in Fig. 6(b) is qualitatively consistent with the measured bandwidth in Fig. 5(b). The ability to separate effects on the individual mirrors of the two-mirror combination permits further refinement of the multilayer coating model that fits the experimental observations.

Both the finite interface thickness and the mismatch of passbands on the two mirrors are likely to contribute to the reduction in the coating bandwidth observed in the Schwarzschild objective. Given the estimated interface thickness of 0.7 nm, the multilayer period offset from the reported values that one needs to match the present measurements consists of both a constant and a linear component, varying along the radius of each substrate. On the primary, the required offset is nearly constant at approximately −0.045 nm. On the secondary, the required period change increases along the substrate radius, reaching a maximum of approximately 0.04 nm. For both mirrors, the offset necessary to fit the data exceeds the estimated measurement uncertainty of ±0.0125 nm.[15] The multilayer periods given by the fit to our interferometry data, by the previously reported reflectometry measurements, and by the coating design are compared in Fig. 7. The transmission

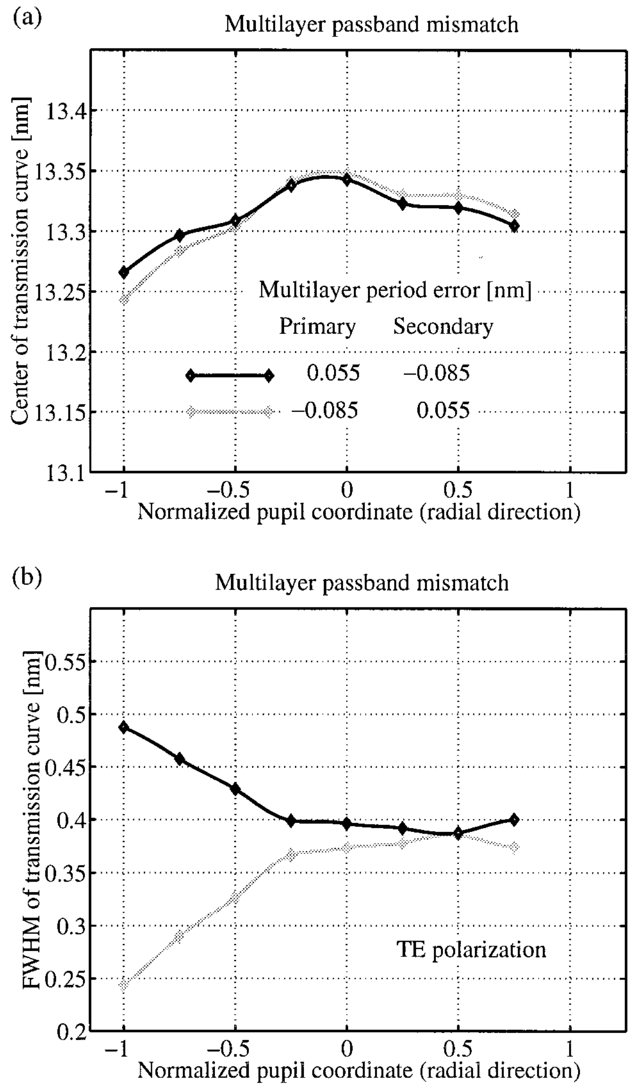

Fig. 6. Calculated passband (a) center and (b) width along the radial direction of the annular aperture of the 10× Schwarzschild objective. Multilayer periods are offset by the indicated constants from those reported in Ref. 5.

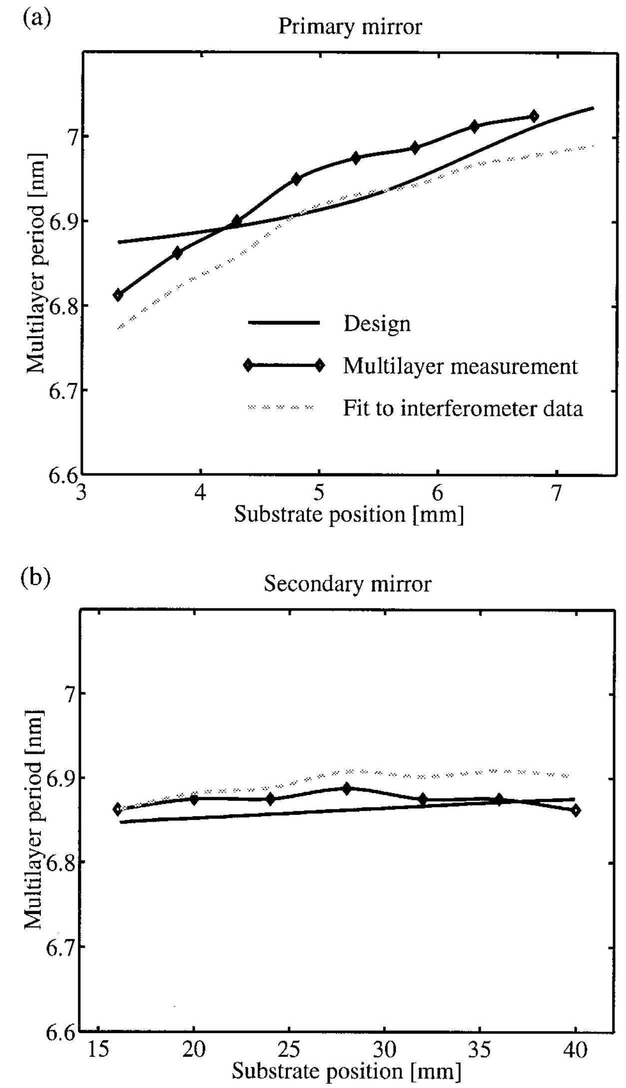

Fig. 7. Period of multilayer reflective coatings on the primary and the secondary mirrors versus the radial position on the substrate. The multilayer design, the measurement from Ref. 5, and the model matching the interferometer data are compared.

characteristics measured on the Schwarzschild optic and those calculated with the present multilayer model closely coincide in both the center and the bandwidth of the transmission curve.

The measured and the calculated transmission characteristics over the aperture of the optic are compared in Fig. 8 for wavelengths ranging from 12.9 to 13.7 nm. The two measurements, shown in Figs. 8(a) and 8(b), correspond to transmission in a 0.08-NA subregion of the annulus near subaperture C and in the 0.07-NA subaperture A, respectively. The calculation over a numerical aperture of 0.08 in Fig. 8(c), which represents the coating model, assumes multilayer coatings with 40 bilayers, a rms interfacial thickness of 0.7 nm, a molybdenum-to-silicon thickness ratio of 0.375, and the coating periods given in Fig. 7. If we neglect the nonuniformities in the illumination of the aperture in the experiment, the coating model shows good consistency with the measurements over the wavelength range considered.

A comparison of the measured and the calculated chromatic phase effects is presented in Fig. 9 for a 0.07-NA subregion of the annular aperture. The chromatic aberrations between adjacent wavelengths, separated by 0.1 nm in the range 12.9 to 13.7 nm, reveal that the model for the coating properties produces good qualitative agreement with measurement not only in the transmission characteristics but also in the measured phase.

Owing to the strong influence of both the interfacial thickness and the multilayer mismatch on the overall coating characteristics, the simplified multilayer model described here represents only one of their possible interactions that fit the measured data. In addition, other potentially significant effects, such as the optical properties of molybdenum and silicon, have not been considered here. The small discrep-

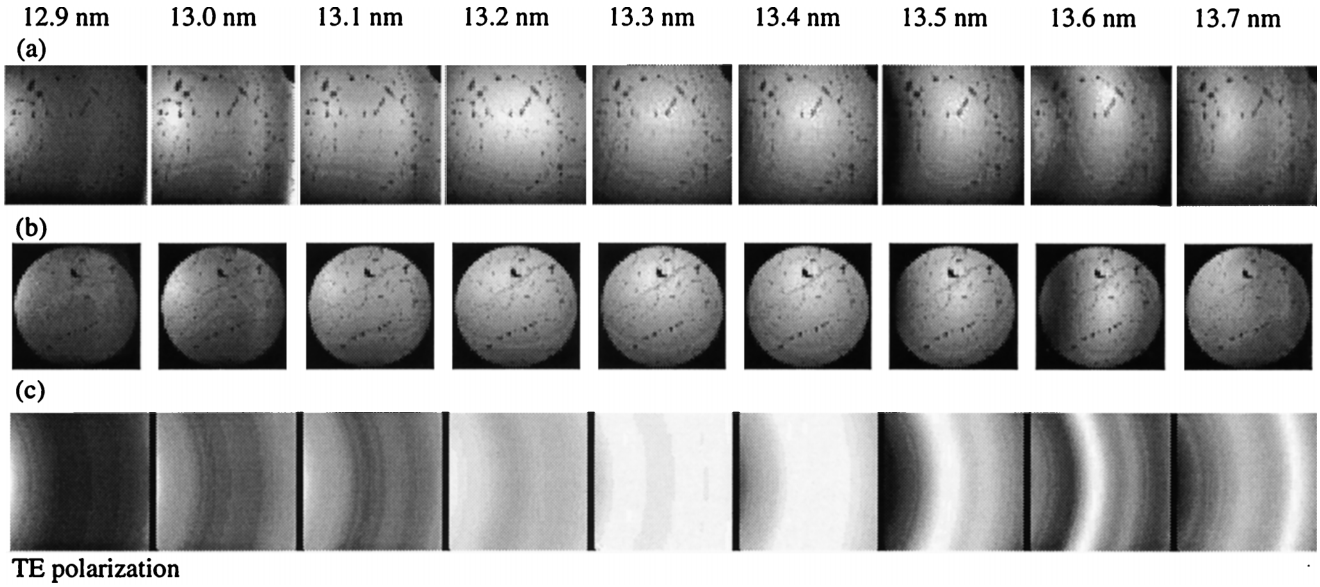

Fig. 8. Measured and calculated transmission through the Schwarzschild optic at several wavelengths. The transmissions measured (a) in a 0.08-NA subregion of the annulus near subaperture C and (b) in the 0.07-NA subaperture A are compared with (c) the transmission calculations that assume coatings with 40 bilayers, a rms interfacial thickness of 0.7 nm, a molybdenum-to-silicon thickness ratio of 0.375, and coating periods given in Fig. 7. In addition to the multilayer properties, the measured images include the intensity profile of the illuminating beam, which can be most clearly observed for the data at 13.3 nm.

ancies found between the measurements of the assembled system and those of the individual mirror substrates demonstrate the need for detailed characterization of the multilayers in EUV optical systems. Measurements of the transmission passband over the aperture of the assembled optical system appear quite valuable for assessing the multilayer coating properties as well as the chromatic effects in the optic.

5. Conclusions

The chromatic vignetting effects caused by the limited passbands of the Mo–Si multilayer coatings in the Schwarzschild optic were studied with interferometry and with transmission measurements at EUV wavelengths. The chromatic phase aberrations and the wavelength-dependent coating transmission variations were observed directly by means of measurements at several wavelengths in the region of the coating passband centered near 13.4 nm. The measurements predicted negligible influence of the chromatic aberrations on the formation of the image in an EUV exposure system. Accounting for the layer interface imperfections and for the variations in the multilayer period over each mirror, good qualitative agreement in both the transmission and

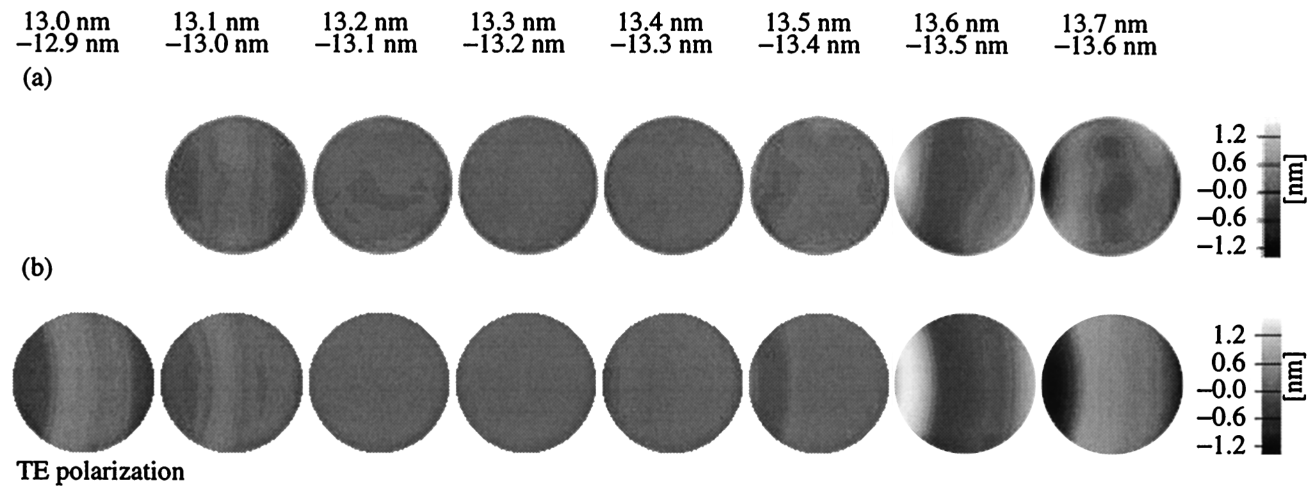

Fig. 9. Measured and calculated chromatic phase effects in the Schwarzschild optic at several wavelengths, represented by the difference in the aberrations at two different wavelengths. (a) The phase effects measured in the 0.07-NA subaperture are compared with (b) the calculations of chromatic aberrations that assume coatings with 40 bilayers, a rms interfacial thickness of 0.7 nm, a molybdenum-to-silicon thickness ratio of 0.375, and coating periods given in Fig. 7.

the phase was obtained between multilayer calculations and the experimental observations. Furthermore, the coating characteristics extracted from the measurements of the two-mirror system were compared with the previously reported coating properties measured on the individual mirrors.

This study was supported by the Semiconductor Research Corporation, the Defense Advanced Research Projects Agency, the Intel Corporation, and the Extreme Ultraviolet Limited Liability Corporation.

References

1. H. Medecki, E. Tejnil, K. A. Goldberg, and J. Bokor, "A phase-shifting point diffraction interferometer," Opt. Lett. **21,** 1526–1528 (1996).
2. E. Tejnil, K. A. Goldberg, S. H. Lee, H. Medecki, P. J. Batson, P. E. Denham, A. A. MacDowell, J. Bokor, and D. T. Attwood, "At-wavelength interferometry for extreme ultraviolet lithography," J. Vac. Sci. Technol. B **15,** 2455–2461 (1997).
3. K. A. Goldberg, E. Tejnil, S. H. Lee, H. Medecki, D. T. Attwood, K. H. Jackson, and J. Bokor, "Characterization of an EUV Schwarzschild objective using phase-shifting point diffraction interferometry," in *Emerging Lithographic Technologies*, D. E. Seeger, ed., Proc. SPIE **3048,** 264–70 (1997).
4. J. H. Underwood, "Reflecting multilayer coatings for EUV projection lithography," in *Extreme Ultraviolet Lithography*, G. D. Kubiak and D. R. Kania, eds., Vol. 4 of OSA Trends in Optics and Photonics Series (Optical Society of America, Washington, D.C., 1996), pp. 162–166.
5. D. L. Windt and W. K. Waskiewicz, "Multilayer facilities required for extreme-ultraviolet lithography," J. Vac. Sci. Technol. B **12,** 3826–3832 (1994).
6. D. A. Tichenor, A. K. Ray-Chaudhuri, G. D. Kubiak, S. J. Haney, K. W. Berger, R. P. Nissen, G. A. Wilkerson, R. H. Stulen, P. H. Paul, R. W. Arling, T. E. Jewell, E. Tejnil, W. C. Sweatt, W. W. Chow, J. E. Bjorkholm, R. R. Freeman, M. D. Himel, A. A. MacDowell, D. M. Tennant, L. A. Fetter, O. R. Wood II, W. K. Waskiewicz, D. L. White, and D. L. Windt, "10× reduction imaging at 13.4 nm," in *Extreme Ultraviolet Lithography*, F. Zernike and D. T. Attwood, eds., Vol. 23 of OSA Proceedings Series (Optical Society of America, Washington, D.C., 1995), pp. 89–97.
7. J. E. Grievenkamp and J. H. Bruning, "Phase-shifting interferometry," in *Optical Shop Testing*, 2nd ed., D. Malacara, ed. (Wiley, New York, 1992), pp. 501–598.
8. R. Soufli and E. M. Gullikson, "Reflectance measurements on clean surfaces for the determination of optical constants in the EUV/soft X-ray region," Appl. Opt. **36,** 5499–5507 (1997); B. L. Henke, E. M. Gullikson, and J. C. Davis, "X-ray interactions: photoabsorption, scattering, transmission, and reflection at $E = 50$–30,000 eV, $Z = 1$–92," At. Data Nucl. Data Tables **54,** 181–342 (1993).
9. T. E. Jewell, "Effect of amplitude and phase dispersion on images in multilayer-coated soft-x-ray projection systems," in *Soft X-Ray Projection Lithography*, J. Bokor, ed., Vol. 12 of OSA Proceedings Series (Optical Society of America, Washington, D.C., 1991), pp. 113–118.
10. J. H. Underwood and T. W. Barbee, Jr., "Layered synthetic microstructures as Bragg diffractors for x rays and extreme ultraviolet: theory and predicted performance," Appl. Opt. **20,** 3027–3034 (1981).
11. E. Spiller, *Soft X-Ray Optics* (SPIE, Bellingham, Wash., 1994), Chap. 7.
12. V. G. Kohn, "On the theory of reflectivity by an x-ray multilayer mirror," Phys. Status Solidi B **187,** 61–70 (1995).
13. A. Caticha, "Reflection and transmission of x rays by graded interfaces," Phys. Rev. B **52,** 9214–9223 (1995).
14. D. L. Windt, R. Hull, and W. K. Waskiewicz, "Interface imperfections in metal/Si multilayers," J. Appl. Phys. **71,** 2675–2678 (1992).
15. D. L. Windt, Bell Laboratories, Room 1D-456, 700 Mountain Avenue, Murray Hill, N.J. 07974 (personal communication, September 1997).